ACS APPLIED MATERIALS & INTERFACES

Research Article

www.acsami.org

Unprecedented CO_2-Promoted Hydrogen Permeation in Ni-$BaZr_{0.1}Ce_{0.7}Y_{0.1}Yb_{0.1}O_{3-\delta}$ Membrane

Shumin Fang,[†] Kyle Brinkman,[‡] and Fanglin Chen[†,*]

[†]Department of Mechanical Engineering, University of South Carolina, Columbia, South Carolina 29208, United States

[‡]Savannah River National Laboratory, Aiken, South Carolina 29808, United States

ABSTRACT: Conventional Ni-$BaCeO_3$-based membranes possess high hydrogen permeation flux but suffer serious flux degradation in CO_2-containing atmosphere because of the formation of $BaCO_3$ insulating layer. In this work, we report a novel Ni-$BaZr_{0.1}Ce_{0.7}Y_{0.1}Yb_{0.1}O_{3-\delta}$ (Ni-BZCYYb) membrane, capable of both high hydrogen permeation flux and stable performance in CO_2-containing atmosphere at 900 °C. Most importantly, the flux is found to be promoted rather than being diminished by CO_2 normally observed for other high temperature proton conductors. The flux enhancement in Ni-BZCYYb membrane is attributed to the increase of moisture content in feed gas. When CO_2 is introduced, the reverse water–gas shift reaction takes place generating H_2O and CO. This work demonstrates that CO_2 can be beneficial rather than detrimental for hydrogen permeation membranes that possess high chemical stability.

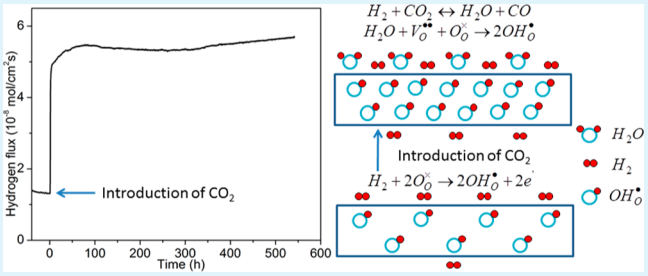

KEYWORDS: *hydrogen permeation, composite membrane, high temperature proton conductor, barium cerate, chemical stability*

1. INTRODUCTION

Hydrogen is not only a key feedstock for the synthesis of important chemicals such as ammonia, methanol, and liquid hydrocarbons, but also a core intermediate for future power generation. Because of concerns about climate change, there is an increasing demand for the development of fossil fuel power plants with carbon capture and storage.[1,2] An attractive alternative to conventional power generation processes is the pre-combustion CO_2 capture/separation option, especially the integrated gasification combined cycle (IGCC) processes, where pure H_2 is separated from a mixture of H_2 and CO_2 before final combustion.[1,3] In conventional hydrogen production through catalytic steam reforming of methane and water-gas shift reaction,[4] hydrogen is separated from the mixture of H_2 and CO_2 through pressure swing adsorption (PSA) process, resulting in high capital cost and energy losses.[5] Therefore, achieving cost-effective and large-scale hydrogen production with feasible CO_2 sequestration has significant economic benefits and contributes to a cleaner environment.[6] A simple and cost-effective alternative process is membrane separation. Although Pd-based alloy membranes show high hydrogen permeation flux, they are expensive, susceptible to cracking, phase transformation, and H_2S poisoning.[5] Composite membranes consisting of a solid-state high temperature proton conductor and an electronic conductor (e.g., nickel) are inexpensive, mechanically rugged, and tolerant to CO and H_2S up to tens of ppm level.[7] Most importantly, they can be applied at elevated temperature, facilitating thermal integration.[8] However, poor chemical stability of the state-of-the-art proton conductors such as $BaZr_{0.1}Ce_{0.7}Y_{0.2}O_{3-\delta}$ (BZCY) in concentrated CO_2 has been a significant obstacle in this application.[9] It is therefore very challenging but extremely important to identify potential high-temperature proton conductors possessing good chemical stability in a concentrated CO_2 environment.

Acceptor-doped $BaCeO_3$ has shown the highest proton conductivities, but suffers from poor chemical stability in H_2O and CO_2.[10−13] In view of this deficiency, numerous $BaCeO_3$-based proton conductors have been explored through cation substitution in order to achieve adequate chemical stability in CO_2 without sacrificing its high proton conductivity.[14−18] The chemical stability of $BaCeO_3$ can be improved by doping Zr at the Ce sites, with the expense of a sharp reduction in proton conductivity and sintering activity.[9,13] The introduction of a small amount of Zn in Ce cites was found to further improve the chemical stability and sintering activity of Zr-doped $BaCeO_3$.[19] Recently, Yang et al. have reported that $BaZr_{0.1}Ce_{0.7}Y_{0.1}Yb_{0.1}O_{3-\delta}$ (BZCYYb) possesses high proton conductivity and high tolerance to CO_2 and H_2S, showing excellent performance as anode materials in solid oxide fuel cells.[20] Consequently, it is anticipated that this material may be potentially used as high performance hydrogen separation membranes. Very recently, an asymmetric Ni-BZCYYb membrane (44 μm thick film on porous substrate) showed remarkably high hydrogen flux; however, the chemical stability in CO_2 has not been investigated.[21]

In this work, we have developed a novel high flux CO_2-tolerant hydrogen permeation membrane based on Ni-

Received: November 17, 2013
Accepted: December 13, 2013
Published: December 13, 2013

$BaZr_{0.1}Ce_{0.7}Y_{0.1}Yb_{0.1}O_{3-\delta}$ (Ni-BZCYYb) cermet. The hydrogen flux increased with the rise of moisture content stemming from the reverse water-gas shift (RWGS) reaction after introduction of CO_2. The stable performance suggests that Ni-BZCYYb possesses excellent chemical stability in CO_2. This work demonstrates that CO_2 can be beneficial rather than detrimental for hydrogen permeation of Ni-BZCYYb membrane.

2. EXPERIMENTAL SECTION

BZCYYb powder was synthesized by a sol-gel combustion method. $Ba(NO_3)_2$ (Alfa Aesar 99%), $Ce(NO_3)_3{\cdot}6H_2O$ (Alfa Aesar 99.5%), $ZrO(NO_3)_2{\cdot}xH_2O$ (Alfa Aesar 99.9%), $Y(NO_3)_3{\cdot}6H_2O$ (Alfa Aesar 99.9%), and $Yb(NO_3)_3{\cdot}6H_2O$ (Alfa Aesar 99.9%) were dissolved in distilled water and titrated by an ethylenediaminetetraacetic acid (EDTA) titrimetric method. Stoichiometric amounts of metal nitrate solution were mixed in a beaker and heated at 80 °C under stirring. EDTA and citric acid were added as complexation agents, with the molar ratio of EDTA/citric acid/total metal cations setting at 1:1.5:1. The pH value of the solution was adjusted by ammonia to around 8. Appropriate amount of ammonium nitrate was then added as a trigger for combustion. The solution was heated under stirring for 2 h followed by heating in a microwave oven until automatic ignition to obtain a white powder. The powder was then calcined at 1100 °C for 5 h to obtain single phase BZCYYb powder. Ni powder (Alfa Aesar, ~325 mesh, 99.8% metal basis) and BZCYYb powder were then mixed in volume ratio of 40:60 using agate mortar and pestle. The mixed powder was pressed in a 20 mm stainless steel die and sintered at 1440 °C for 20 h in 5% H_2/N_2 to obtain Ni-BZCYYb dense membrane. The sintered membrane is conductive at room temperature, suggesting that a connected network of Ni is formed that ensures adequate electronic conductivity. For the chemical stability test in CO_2, Ni-BZCYYb membranes were polished first with 600 and 1200 grits silicon carbide sandpapers, and then with 9, 3, and 1 μm diamond suspension on a Bluehler polisher. The membranes were thermally etched at 1400 °C for 2 h in 5% H_2 before annealing in 20% H_2, 20% CO_2, and 60% N_2 at 900 °C for 200 h.

The membrane was tested in a set-up for hydrogen permeation flux measurement (shown in Figure 1). Both surfaces of sintered membrane were polished with silicon carbide sandpapers (120, 320, 600 grits) before the hydrogen permeation measurement. The Ni-BZCYYb membrane was sealed using two glass rings to two vertical alumina tubes. To prevent exposure of the membrane to air, the edge of the membrane was first covered with glass powder well-dispersed in terpineol, dried, and then covered by ceramic-glass sealant (Aremco C552). The sealing was achieved by heating at 90, 130, 230, 1000 °C for 3, 3, 3, and 1 h, respectively. The feed gas is a mixture of H_2 balanced with He (airgas, 99.9993%) and N_2 (airgas, 99.9993%)/CO_2 (airgas, 99%) with a total flow rate of 100 mL/min. The feed gases including H_2, N_2, He were controlled by mass flow controllers (Apex Vacuum Schoonover Inc), mixed in a 500 mL 4-neck glass flask. The relative humidity in the exhaust of the feed side was continuously monitored by a humidity & temperature transmitter (Vaisala HMT338). The moisture content was calculated from the relative humidity and the saturated vapor pressure at the corresponding temperature. The sweep gas was 20 mL/min N_2 (airgas, 99.9993%). The composition of the exhaust from the feed side and sweep side was analyzed by a gas chromatograph (GC, Agilent 7890A) equipped with two thermal conductivity detectors using ultra carrier grade N_2 and He as carrier gases, respectively. The GC was regularly calibrated by standard gas (Airgas). The flow rate of the exhaust from the sweep side was measured by a digital flow meter (Agilent ADM2000). The leakage through incomplete sealing was checked by measuring He concentration in the sweep gas. The leakage detected was less than 1% in all cases, suggesting that an effective sealing was obtained.

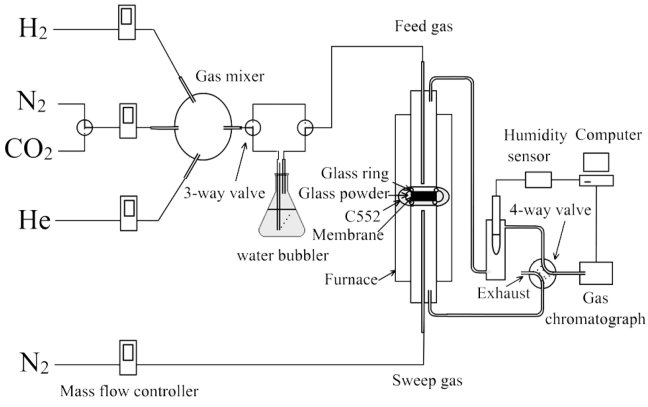

Figure 1. Schematic of set-up for hydrogen permeation flux measurement.

X-ray diffraction (XRD, Rigaku D/Max 2100, with Cu Kα radiation) analysis was used to identify the phases present in the powder and pellets. Field-emission scanning electronic microscopy (FESEM, Zeiss ultra plus) was used to study the microstructure of the Ni-BZCYYb membranes. Raman spectra were obtained with a Nomadic Raman Microscope (Bayspec Inc). The 785 nm line of a diode laser was used as the exciting radiation.

3. RESULTS AND DISCUSSION

3.1. Theoretical Background. For the Ni-BZCYYb membrane, hydrogen can diffuse through the BZCYYb ceramic phase in the form of hydroxide defects or through the Ni metal phase in the form of hydrogen atoms. The reactions are as follows

$$1/2H_2(g) + O_O^{\times} = OH_O^{\bullet} + e' \quad (1)$$

$$1/2H_2(g) = H(\text{dissolved}) \quad (2)$$

In both cases, the driving force for hydrogen permeation is the hydrogen partial pressure gradient. The diffusion of protons in BZCYYb requires the transfer of equal amount of electrons. Although the electronic conductivity of BZCYYb is very low, the electrons can be transferred through Ni which has a very high electronic conductivity (e.g., 1.43×10^5 S/cm at 20 °C). In this sense, proton conductivity is minor compared with electronic conductivity in the Ni-BZCYYb composite membrane. The hydrogen permeation process in a Ni-$BaCe_{0.8}Y_{0.2}O_{3-\delta}$ (Ni-BCY) membrane is bulk-controlled until 80 μm,[22] and therefore the Wagner equation is applicable. As Ni-BCY and Ni-BZCYYb are similar in composition, we assume that the Wagner equation can also be applied in Ni-BZCYYb since the Ni-BZCYYb composite membrane has a thickness of at least 0.40 mm in this study. The application of the Wagner equation to a proton conductor whose minor defects are protons yields

$$J = \frac{RT\sigma\Delta p^{1/2}}{2F^2L} \quad (3)$$

where J, R, T, σ, $\Delta p^{1/2}$, F, and L are the flux, ideal gas constant, temperature, proton conductivity, the difference of the square roots in hydrogen partial pressure between feed and sweep gases, Faraday constant, and membrane thickness, respectively.[8] In the Ni phase, according to Fick's first law and the Sievert's law

$$J = \frac{P\Delta p^{1/2}}{L} \quad (4)$$

dx.doi.org/10.1021/am405169d | ACS Appl. Mater. Interfaces 2014, 6, 725−730

where P is permeability of hydrogen in Ni.[23] Considering the dilution effect in composite, the flux of Ni-BZCYYb membrane can be determined through

$$J = \alpha\frac{RT\sigma\Delta p^{1/2}}{2F^2L} + \beta\frac{P\Delta p^{1/2}}{L} \quad (5)$$

Here, α and β are dilution coefficients ($\alpha, \beta < 1$). According to the eq 5, the flux increases with increasing temperature, proton conductivity of BZCYYb, and permeability of hydrogen in nickel. It is also proportional to the difference in the square root of hydrogen partial pressure between feed and sweep gases ($\Delta p^{1/2}$) and the reciprocal of the thickness of the Ni-BZCYYb membrane.

3.2. Permeation Flux in Different Conditions. Figure 2 shows the dependence of hydrogen flux of a 0.4 mm thick Ni-BZCYYb membrane on $\Delta p^{1/2}$. Obviously, the hydrogen flux is proportional to $\Delta p^{1/2}$ in the measured temperature region, which agrees well with eq 5, indicating that the hydrogen permeation is determined by bulk diffusion process, because eq 5 is only applicable in this condition. When the membrane is thinner, the hydrogen permeation process may be controlled by the surface exchange kinetics. However, similar relationship between flux and $\Delta p^{1/2}$ is observed in an asymmetric Ni-BZCYYb membrane (44-μm-thick film on porous substrate),[21] suggesting that the permeation process is still controlled by bulk diffusion process even in such a thin membrane. The relationship in eq 5 can be used to predict the flux at high pressures. The outlet gas from the typical methane steam reforming process has a rather high pressure (~30 bar) and the hydrogen flux extrapolated from the current study at 900 °C can be as high as 1.0×10^{-6} mol/(cm^{2}s). Figure 2 also shows that the flux increases with moisture content and temperature. This also agrees well with eq 5. It has been well accepted that dissociative adsorption of water forms additional protonic defects, resulting in an increase in proton conductivity of perovskite-type proton conductors.[14,18,24] Moreover, both the proton conductivity in BZCYYb (σ) and hydrogen permeability in Ni (P) increase with temperature. Therefore, the flux increases with temperature and moisture content.

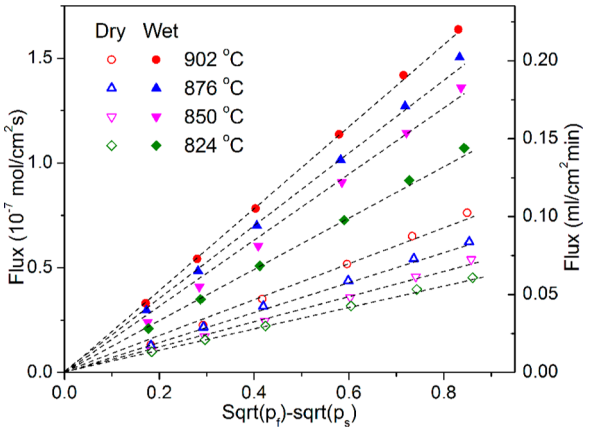

Figure 2. Dependence of hydrogen permeation flux of a 0.4 mm thick Ni-BZCYYb membrane on the difference of square root of hydrogen partial pressure between feed and sweep gas. The humidity in dry and wet atmosphere is 0.01 and 3%, respectively.

Figure 3 compares the hydrogen permeation flux of a 0.4 mm thick Ni-BZCYYb membrane at ~900 °C with the literature data of Ni-$BaZr_{0.1}Ce_{0.7}Y_{0.2}O_{3-\delta}$ (Ni-BZCY) membrane. In wet H_2 (moisture content = 3 vol%), the flux of Ni-BZCYYb membrane increased by a factor of 4.9 to 1.6×10^{-7} mol/(cm^{2}s) when hydrogen content in the feed gas increased from 4 to 80%. The increased hydrogen flux was attributed to an enhanced driving force for hydrogen permeation. Because of the difference in sample thicknesses from the different studies, it is not valid to directly compare the hydrogen flux. It has been reported that the permeation process of Ni-BCY membrane is bulk controlled if the sample thickness is more than 80 μm and the flux is proportional to the reciprocal of membrane thickness according to eq 5. Assuming that the Ni-BZCY and Ni-$BaCe_{0.6}Zr_{0.2}Nd_{0.2}O_{3-\delta}$ (Ni-BCZN) membranes also behaves similarly, the flux from the different membranes can be normalized to that of a 0.4 mm thick membrane. It is noted that the flux of Ni-BZCYYb is very close to that of Ni-BZCY reported by Yan et al.[25] and Fang et al.,[7] and significantly higher than that of Ni-BCZN membrane.[26] In general, the flux of Ni-BZCYYb membrane is comparable to that of the state-of-the-art Ni-BZCY membrane. The flux is expected to be further improved through the fabrication of asymmetric membranes and hollow fibers.[21,27] The high permeability and low cost of Ni-BZCYYb membrane makes it extremely promising in practical application for hydrogen separation, providing that it meets the requirement of adequate chemical stability in CO_2-containing atmospheres.

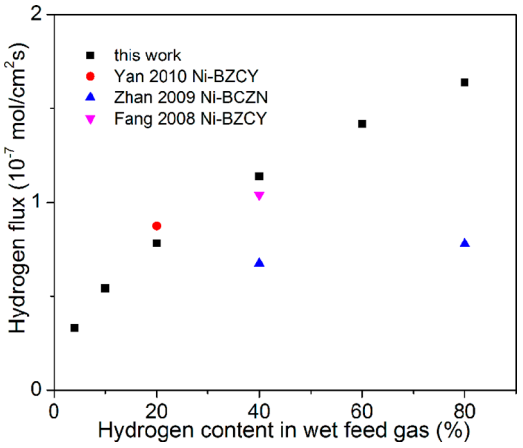

Figure 3. Dependence of hydrogen flux of a 0.4 mm thick membrane on hydrogen content in feed gas containing 3% H_2O. Literature data are added for the ease of comparison.

3.3. Chemical Stability in CO_2. To evaluate the chemical stability in CO_2, we analyzed the phase composition and microstructure of Ni-BZCYYb membrane before and after annealing in 20% H_2, 20% CO_2, and 60% N_2 for 200 h at 900 °C. Figure 4 shows the XRD patterns of fresh and annealed BZCYYb powder and Ni-BZCYYb membrane surfaces. The XRD patterns of fresh and annealed powder and membrane only showed XRD peaks corresponding to BZCYYb or Ni phases, suggesting that Ni and BZCYYb phases were obtained after sintering in reducing atmosphere and remained stable in 20% CO_2 at 900 °C. On the surface SEM images of fresh and annealed Ni-BZCYYb samples (Figure 5), Ni particles (2−10 μm) were embedded in the dense BZCYYb ceramic matrix. There has been no microstructure change for the annealed membrane, further confirming the chemical stability of Ni-BZCYYb membrane in CO_2-containing atmospheres at 900 °C.

dx.doi.org/10.1021/am405169d | ACS Appl. Mater. Interfaces 2014, 6, 725−730

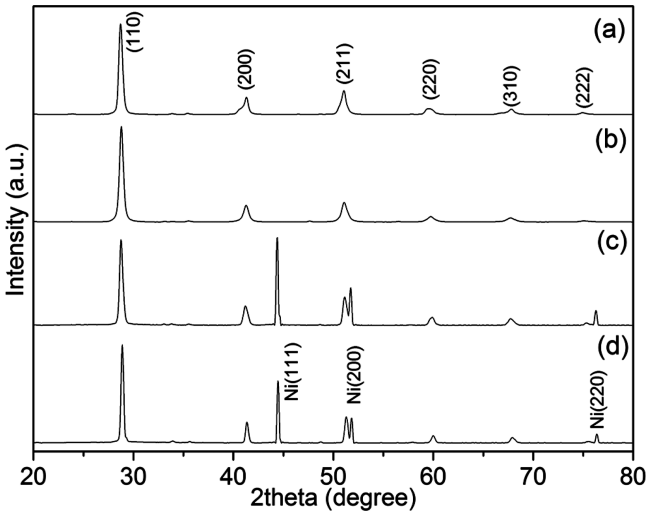

Figure 4. XRD patterns of (a, b) BZCYYb powder and (c, d) Ni-BZCYYb membranes (a, c) before and (b, d) after annealing in 20% H_2, 20% CO_2, and 60% N_2 at 900 °C for 200 h.

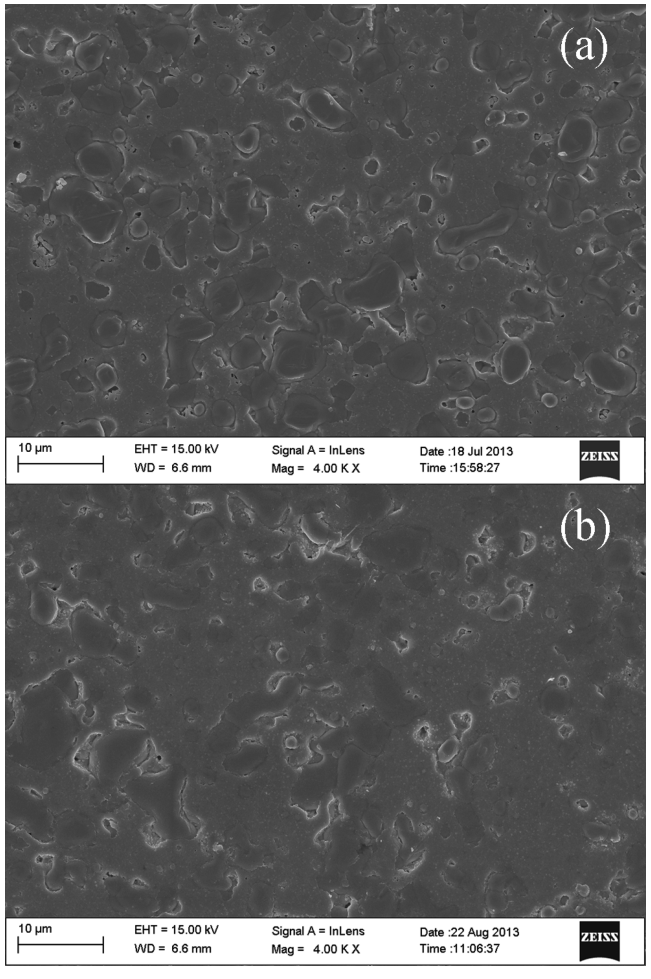

Figure 5. SEM images of Ni-BZCYYb membrane (a) before and (b) after annealing in 20% H_2, 20% CO_2, and 60% N_2 at 900 °C for 200 h.

To determine the performance stability of the membrane in CO_2-containing atmosphere, we tested the membrane in H_2 with different concentration of CO_2. Figure 6 shows the time dependence of the hydrogen permeation flux of a 0.75 mm

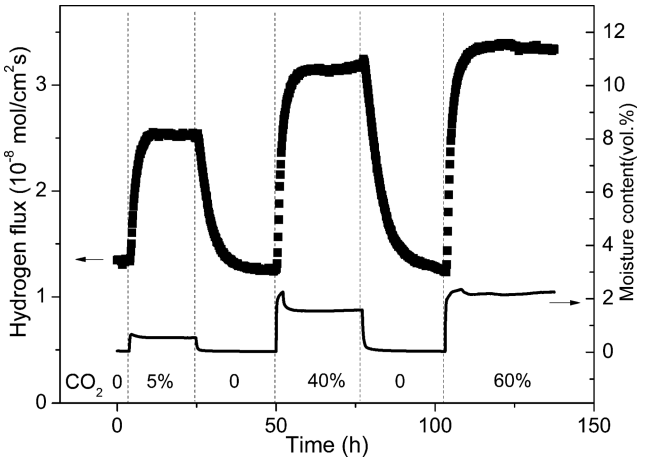

Figure 6. Time dependence of hydrogen permeation fluxes of a 0.75 mm thick Ni-BZCYYb membrane and absolute humidity in feed gas passing through the reactor. The feed gas consisted of 20 mL/min H_2, x mL/min CO_2, and 80 − x mL/min He.

thick Ni-BZCYYb membrane and moisture content in the feed gas when 0, 5, 40, and 60 vol% CO_2 was introduced. At the beginning of the experiment, the feed gas was 20% H_2 balanced with N_2 and He with a moisture content of only 0.03% (due to residual moisture in the gas line), resulting in a hydrogen flux of 1.3×10^{-8} mol/(cm^2 s). However, when 5, 40, and 60 vol % CO_2 was introduced into the feed gas, the moisture content increased to ∼0.5, 1.6, and 2.2 vol% and the flux increased to 2.5, 3.2, and 3.4×10^{-8} mol/(cm^2 s), respectively. When CO_2 was removed from the feed gas, the moisture content decreased rapidly to ∼0.03% and the flux decreased to 1.3×10^{-8} mol/(cm^2 s), indicating that the process was reversible. The increase in water partial pressure in the feed gas upon introduction of CO_2 was due to the reverse water−gas shift (RWGS) reaction

$$H_2(g) + CO_2(g) = H_2O(g) + CO(g) \quad (6)$$

The RWGS reaction consumes H_2 and CO_2, and generates an equal amount of H_2O and CO. The CO concentration in the outlet of the feed gas analyzed by gas chromatography was correlated well with that of H_2O measured by humidity sensor, indicating good agreement with the proposed reaction 6. Under thermodynamic equilibrium, the increase of CO_2 concentration will shift the reaction towards the right, thus increasing the H_2O concentration. The flux of the Ni-BZCYYb membrane increased with increasing moisture content in the feed stream, as indicated from Figure 2. Therefore, it can be concluded that CO_2 introduced into H_2 in the feed gas stream can generate water, leading to an increase in proton conductivity and thus hydrogen permeation flux.

It is noticeable that the extent of performance enhancement decreases significantly with further increasing CO_2 and moisture content. In Kröger−Vink notation, the dissociation reaction of water into perovskite lattice can be written as[14]

$$H_2O + V_O^{\bullet\bullet} + O_O^{\times} = 2OH_O^{\bullet} \quad (7)$$

The concentration of protonic defects follows following relationship

$$[OH_O^{\bullet}] = K^{1/2}[V_O^{\bullet\bullet}]^{1/2}[O_O^{\times}]p^{1/2} \quad (8)$$

where K and p are the equilibrium constant of reaction 7 and moisture partial pressure, respectively.[14] The concentration of

protonic defects is proportional to the square root of oxygen vacancy concentration and moisture partial pressure. The square root function levels off after a fast initial increase, and thus the concentration of protonic defects is expected to level off with increasing moisture partial pressure, assuming that the oxygen vacancy concentration is fixed. Moreover, as moisture partial pressure increases, water is dissociated in the lattice consuming oxygen vacancies, leading to decrease in the amount of available oxygen vacancies. Therefore, the protonic defect concentration and the proton conductivity of BZCYYb increases slowly with further increasing moisture content. In addition, the reaction 6 consumes H_2 when producing H_2O, and the effect becomes more obvious when CO_2 content becomes higher. Although this effect is minor (e.g., the flux decreases from 7.8 to 7.4 × 10^{-8} mol/(cm^2 s) when hydrogen content decreases from 20 to 18% in Figure 3), it also contributes to the slowdown of performance increase. Therefore, the flux enhancement becomes less prominent with further increasing CO_2 and H_2O content in Figure 6.

To evaluate the long-term stability of Ni-BZCYYb membrane in CO_2, we tested a 0.4 mm thick membrane in feed gas containing 20% H_2, 20% CO_2, and 60% N_2 for 540 h at 900 °C. Figure 7a shows the time dependence of hydrogen flux. The membrane shows very stable performance during the long-term test, confirming that Ni-BZCYYb membrane possesses excellent stability in the presence of CO_2. It has been reported that the performance of Ni−$BaCe_{0.8}Y_{0.2}O_{3-\delta}$ and Ni−$BaZr_{0.1}Ce_{0.7}Y_{0.2}O_{3-\delta}$ membranes in wet (3 vol% H_2O) 4% H_2/He was 1 or 2 times higher than that in dry 4% H_2 between 600 and 900 °C.[13] Unfortunately, those membranes suffered serious performance degradation (between 100 and 45%) when exposed to 30 vol % CO_2-containing atmosphere at 900 °C. Although the performances of $SrCe_{0.75}Zr_{0.2}Tm_{0.05}O_{3-\delta}$ at 900 °C in 20% H_2 and 20% CO_2 first increased from 2.2 × 10^{-8} to 5.5 × 10^{-8} mol/(cm^2 s), it gradually decreased to 2.2 × 10^{-8} mol/(cm^2 s) in 70 h.[28] Unlike the membranes reported in the literature, Ni-BZCYYb membrane shows a stable and improved performance in the presence of highly concentrated CO_2, suggesting that it possess excellent chemical stability in concentrated CO_2 at 900 °C. These results show that Ni-BZCYYb membrane material is very promising for applications in hydrogen separation in the presence of CO_2 and highlight the important potential that proton-conducting ceramic materials have for future membrane separation processes. There are several parameters that may affect the chemical stability of Ni-BZCYYb membrane. First, the reaction between CO_2 and $BaCeO_3$ is thermodynamically favored at low temperature. At 900 °C, the critical CO_2 partial pressure for the reaction between CO_2 and $BaCe_{0.9}Y_{0.1}O_{3-\delta}$ is ∼27% based on results from thermogravimetric measurements.[12] Therefore, the chemical stability of $BaCeO_3$ itself is reasonably high under such condition. Secondly, it is well-known that Zr-doping in $BaCeO_3$ improves its chemical stability.[9,13] Thirdly, Yb-doping is also helpful in improving the chemical stability of $BaCeO_3$ against CO_2.[29] Fourthly, the reverse water gas shift reaction observed in this study is expected to reduce CO_2 concentration in the feed stream, leading to improved chemical stability of the Ni-BZCYYb membrane. Finally, the BZCYYb powder was made through a wet-chemical process in this study, and its chemical composition homogeneity should be much better than that of BZCY prepared by solid state reaction method.[13] The chemical stability of Zr-doped BCY with high composition homogeneity has been reported to be much better than that with low composition homogeneity.[30] Consequently, the excellent chemical stability of the Ni-BZCYYb membrane in CO_2-containing environment observed in this study should be the combined effects of the above factors.

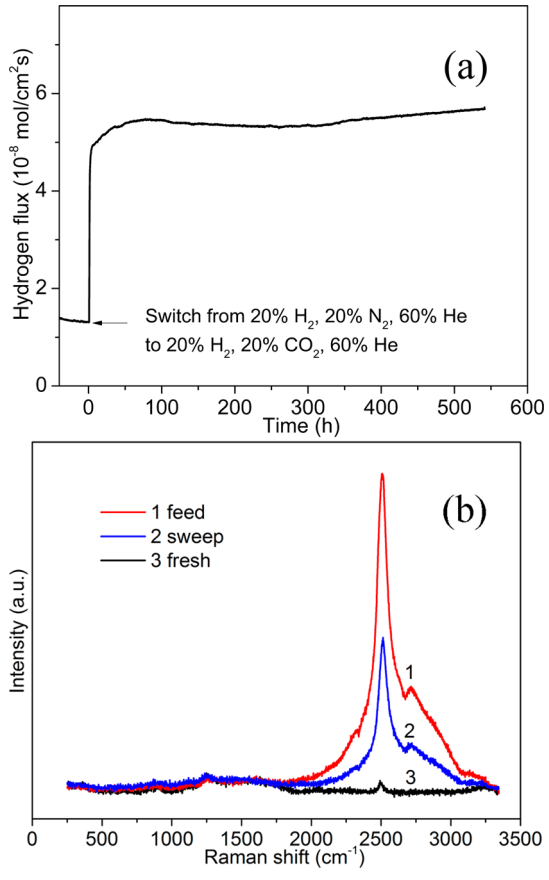

Figure 7. (a) Time dependence of hydrogen flux and moisture content in 20% H_2, 20% CO_2, and 60% He at 900 °C. Membrane thickness is 0.4 mm. (b) Raman spectra of Ni-BZCYYb membrane before and after test in 20% CO_2 at 900 °C for 540 h.

In Figure 7b, the Raman spectra of fresh and long-term tested membrane show no sign of formation of CO_3^{2-} (peaks appear at ∼700 and 1064 cm^{-1}).[31] The most significant change is that the intensity of the peak (∼2500 cm^{-1}) dramatically increases after the test, especially for the feed side surface. This peak corresponds to the O−H stretching mode which originates from dissociation of water into the perovskite bulk phase.[32−34] The feed side surface was directly exposed to water and thus the intensity was the highest. Only a fraction of the O−H was able to diffuse through the membrane to the sweep side and thus the intensity was lower. The fresh membrane was sintered in a dry hydrogen atmosphere and the peak intensity was negligible. This also suggests that the exposure to H_2 and CO_2 can improve the proton conductivity of BZCYYb phase.

The effect of CO_2 on the performance of membranes based on perovskite oxides has been widely investigated, especially for oxygen permeation membranes such as $SrCo_{0.8}Fe_{0.2}O_{3-\delta}$ and $Ba_{0.5}Sr_{0.5}Co_{0.8}Fe_{0.2}O_{3-\delta}$.[35−42] Because these oxides contain alkaline earth metal elements while CO_2 is an acidic gas, they have the tendency to react leading to the decomposition of perovskite phases and consequently performance degradation. When performance degradation and phase decomposition are observed together after the introduction of CO_2, the former is

naturally attributed to the latter. This method works well for oxygen permeation membranes and apparently also applies to the hydrogen permeation membrane based on perovskite oxide like BZCY.[9,13] However, typical gases such as O_2, N_2, and He used in the oxygen permeation membranes are inert with CO_2, whereas H_2 involved in the hydrogen permeation membranes can react with CO_2 through the RWGS reaction to change H_2O content in the environment. Such differences have not been taken into consideration in the previous studies. The RWGS reaction has been found to play an important role in the performance of Ni-BZCYYb membrane in this study. It was demonstrated that Ni-BZCYYb membrane possesses an enhanced chemical stability in CO_2-containing environments compared with existing membrane material systems.

4. CONCLUSIONS

In summary, novel Ni-BZCYYb membrane has demonstrated stable performance in highly concentrated CO_2 at 900 °C. Unlike the Ni-BZCY or Ni-BCY membrane which suffers significant performance degradation even in 20% CO_2, the Ni-BZCYYb membrane has demonstrated stable performance even in 60% CO_2 at 900 °C. The introduction of CO_2 in the feed gas stream has been found to enhance the hydrogen flux by increasing the moisture content through the RWGS reaction. These results show that Ni-BZCYYb membrane is very promising for applications in hydrogen separation in the presence of concentrated CO_2, which plays an essential role in future hydrogen production for chemical and power generation with carbon capture and storage.

AUTHOR INFORMATION

Corresponding Author

*Tel: +1-803-777-4875. Fax: +1-803-777-0106. E-mail: chenfa@cec.sc.edu.

Notes

The authors declare no competing financial interest.

ACKNOWLEDGMENTS

We gratefully acknowledge the financial support from the HeteroFoaM Center, an Energy Frontier Research Center funded by the U.S. Department of Energy, Office of Science, Basic Energy Sciences under Award DESC0001061 and the DOE Office of Nuclear Energy's Nuclear Energy University Programs.

REFERENCES

(1) Smart, S.; Lin, C. X. C.; Ding, L.; Thambimuthu, K.; da Costa, J. C. D. *Energy Environ. Sci.* **2010**, *3*, 268−278.
(2) Zhang, L.; Xu, N.; Li, X.; Wang, S.; Huang, K.; Harris, W. H.; Chiu, W. K. S. *Energy Environ. Sci.* **2012**, *5*, 8310−8317.
(3) Pires, J. C. M.; Martins, F. G.; Alvim-Ferraz, M. C. M.; Simoes, M. *Chem. Eng. Res. Des.* **2011**, *89*, 1446−1460.
(4) Muradov, N. Z.; Veziroglu, T. N. *Int. J. Hydrogen Energy* **2005**, *30*, 225−237.
(5) Lu, G. Q.; da Costa, J. C. D.; Duke, M.; Giessler, S.; Socolow, R.; Williams, R. H.; Kreutz, T. *J. Colloid Interface Sci* **2007**, *314*, 589−603.
(6) Jacobson, M. Z.; Colella, W. G.; Golden, D. M. *Science* **2005**, *308*, 1901−1905.
(7) Fang, S. M.; Bi, L.; Wu, X. S.; Gao, H. Y.; Chen, C. S.; Liu, W. *J. Power Sources* **2008**, *183*, 126−132.
(8) Norby, T.; Haugsrud, R. In *Nonporous Inorganic Membranes for Chemical Processing*, 1st ed.; Sammells, A. F., Mundschau, M. V., Eds.; Wiley: Weinheim, Germany, 2006; p 1.
(9) Zuo, C. D.; Lee, T. H.; Song, S. J.; Chen, L.; Dorris, S. E.; Balachandran, U.; Liu, M. L. *Electrochem. Solid-State lett.* **2005**, *8*, J35−J37.
(10) Bhide, S. V.; Virkar, A. V. *J. Electrochem. Soc.* **1999**, *146*, 2038−2044.
(11) Hibino, T.; Hashimoto, A.; Suzuki, M.; Sano, M. *J. Electrochem. Soc.* **2002**, *149*, A1503−A1508.
(12) Zakowsky, N.; Williamson, S.; Irvine, J. T. S. *Solid State Ionics* **2005**, *176*, 3019−3026.
(13) Zuo, C. D.; Dorris, S. E.; Balachandran, U.; Liu, M. L. *Chem. Mater.* **2006**, *18*, 4647−4650.
(14) Kreuer, K. D. *Ann. Rev. Mater. Res.* **2003**, *33*, 333−359.
(15) Norby, T. *Nature* **2001**, *410*, 877−878.
(16) Fang, S. M.; Bi, L.; Yan, L. T.; Sun, W. P.; Chen, C. S.; Liu, W. *J. Phys. Chem. C* **2010**, *114*, 10986−10991.
(17) Haugsrud, R.; Norby, T. *Nat. Mater.* **2006**, *5*, 193−196.
(18) Zuo, C. D.; Lee, T. H.; Dorris, S. E.; Balachandran, U.; Liu, M. L. *J. Power Sources* **2006**, *159*, 1291−1295.
(19) Tao, S. W.; Irvine, J. T. S. *Adv. Mater.* **2006**, *18*, 1581−1584.
(20) Yang, L.; Wang, S. Z.; Blinn, K.; Liu, M. F.; Liu, Z.; Cheng, Z.; Liu, M. L. *Science* **2009**, *326*, 126−129.
(21) Liu, M.; Sun, W.; Li, X.; Feng, S.; Ding, D.; Chen, D.; Liu, M.; Park, H. C. *Int. J. Hydrogen Energy* **2013**, *38*, 14743−14749.
(22) Song, S. J.; Moon, J. H.; Lee, T. H.; Dorris, S. E.; Balachandran, U. *Solid State Ionics* **2008**, *179*, 1854−1857.
(23) Mundschau, M. V. In *Inorganic Membranes for Energy and Environmental Applications*, 1st ed.; Bose, A. C., Eds.; Springer: New York, 2009; p 146.
(24) Cai, M. Y.; Liu, S.; Efimov, K.; Caro, J.; Feldhoff, A.; Wang, H. H. *J. Membr. Sci.* **2009**, *343*, 90−96.
(25) Yan, L.; Sun, W.; Bi, L.; Fang, S.; Tao, Z.; Liu, W. *J. Alloys Compd.* **2010**, *508*, L5−L8.
(26) Zhan, S. J.; Zhu, X. F.; Wang, W. P.; Ji, B. F.; Yang, W. S.; Lin, L. W. *Chinese J. Catal.* **2009**, *30*, 986−990.
(27) Tan, X.; Song, J.; Meng, X.; Meng, B. *J. Eur. Ceram. Soc.* **2012**, *32*, 2351−2357.
(28) Kniep, J.; Lin, Y. S. *Ind. Eng. Chem. Res.* **2010**, *49*, 2768−2774.
(29) Matsumoto, H.; Kawasaki, Y.; Ito, N.; Enoki, M.; Ishihara, T. *Electrochem. Solid-State lett.* **2007**, *10*, B77−B80.
(30) Haile, S. M.; Staneff, G.; Ryu, K. H. *J. Mater. Sci.* **2001**, *36*, 1149−1160.
(31) Tu, C. S.; Chien, R. R.; Schmidt, V. H.; Lee, S. C.; Huang, C. C. *J. Phys.−Condens. Mater.* **2012**, *24*, 155403−155408.
(32) Salzmann, C. G.; Kohl, I.; Loerting, T.; Mayer, E.; Hallbrucker, A. *J. Phys. Chem. B* **2003**, *107*, 2802−2807.
(33) Diniz, R.; Dantas, M. S.; Fernandes, N. G.; Sansiviero, M. T. C. *Spectrochim. Acta A* **2007**, *67*, 372−377.
(34) Grimaud, A.; Bassat, J. M.; Mauvy, F.; Simon, P.; Canizares, A.; Rousseau, B.; Marrony, M.; Grenier, J. C. *Solid State Ionics* **2011**, *191*, 24−31.
(35) Nomura, K.; Ujihira, Y.; Hayakawa, T.; Takehira, K. *Appl. Catal. A* **1996**, *137*, 25−36.
(36) Benson, S. J.; Waller, D.; Kilner, J. A. *J. Electrochem. Soc.* **1999**, *146*, 1305−1309.
(37) Shao, Z. P.; Yang, W. S.; Cong, Y.; Dong, H.; Tong, J. H.; Xiong, G. X. *J. Membr. Sci.* **2000**, *172*, 177−188.
(38) Homonnay, Z.; Nomura, K.; Juhász, G.; Gál, M.; Sólymos, K.; Hamakawa, S.; Hayakawa, T.; Vértes, A. *Chem. Mater.* **2002**, *14*, 1127−1135.
(39) Yi, J. X.; Feng, S. J.; Zuo, Y. B.; Liu, W.; Chen, C. S. *Chem. Mater.* **2005**, *17*, 5856−5861.
(40) Arnold, M.; Wang, H. H.; Feldhoff, A. *J. Membr. Sci.* **2007**, *293*, 44−52.
(41) Yan, A. Y.; Maragou, V.; Arico, A.; Cheng, M.; Tsiakaras, P. *Appl. Catal. B* **2007**, *76*, 320−327.
(42) Yan, A.; Cheng, M.; Dong, Y. L.; Yang, W. S.; Maragou, V.; Song, S. Q.; Tsiakaras, P. *Appl. Catal. B* **2006**, *66*, 64−71.